Two-dimensional weak-localization effect in the stage-4 $MoCl_5$ graphite intercalation compound

Masatsugu Suzuki and Itsuko S. Suzuki
Department of Physics, State University of New York at Binghamton, Binghamton, New York 13902-6016

Keiko Matsubara*
Department of Electrical Engineering, College of Science and Technology, Nihon University, Chiyoda-ku, Tokyo 101-8308, Japan

Ko Sugihara
College of Pharmacy, Nihon University, Funabashi, Chiba 274-8555, Japan

(Received 6 August 1999)

The c-axis resistivity $\rho_c(H,T)$ of a stage-4 $MoCl_5$ graphite intercalation compound between 1.9 and 50 K has been measured with and without an external magnetic field along the c axis ($0 \leq H \leq 44$ kOe). The interior graphite (G) layers form a bottleneck to the c-axis conduction. The T and H dependences of ρ_c are mainly determined from that of the bottleneck resistivity which is proportional to the in-plane resistivity of interior graphite layers. An observed logarithmic behavior of ρ_c in the form of $\ln(T)$ and $\ln(H)$ indicates that the two-dimensional weak localization occurs in the interior G layers. The T and H dependences of the in-plane conductivity derived from ρ_c are well described by a scaling function of $H\tau_\varepsilon$ at low T and low H, where τ_ε is the characteristic relaxation time for inelastic scattering and is dependent on $T(\tau_\varepsilon \approx T^{-0.2})$.

I. INTRODUCTION

In the past two decades c-axis electrical resistivity measurements have been carried out for various kinds of graphite intercalation compounds (GIC's) with a staging structure along the c axis.[1–11] Models of the c-axis conduction mechanism have been proposed to explain these results.[12–17] The overlapping of the wave functions of carriers over adjacent G layers in GIC's is crucial for the c-axis conduction. Depending on the degree of the overlap the following two models are proposed: the two-dimensional (2D) band model and the three-dimensional (3D) band model. The 2D band model may be appropriate for acceptor GIC's where the intercalate layers are insulating. There is no overlapping of the wave function over nearest-neighbor G layers: carriers are localized in each G layer. The c-axis conduction can occur via the hopping of carriers between G layers through a conduction-channel (conduction-path) Hamiltonian.

Suzuki *et al.*[9] reported the temperature (T) dependence of the c-axis resistivity (ρ_c) and longitudinal magnetoresistance [cL-MR($H\|c$)] of stage 2–6 $MoCl_5$ GIC's, where H is an external magnetic field. They found (i) a metallic behavior in stage 2; (ii) a logarithmic behavior at low T in stages 3 and 4, as well as a negative magnetoresistance (N-MR) at low T and weak H in stages 3–5, and (iii) a semiconductorlike behavior in high stages (5 and 6). They have shown that these results can be qualitatively explained within the framework of a 2D band model with a hopping conduction mechanism. The logarithmic behavior and N-MR are due to a 2D weak-localization effect (WLE).

Matsubara *et al.*[11] also reported experimental results of the a-axis resistivity (ρ_a), a-axis transverse magnetoresistance [aT-MR($H\|c$)], and the c-axis transverse magnetoresistance [cT-MR($H\|a$)] for stage 2–6 $MoCl_5$ GIC's. For stages 2–5, ρ_a shows a metalliclike T dependence, and exhibits no logarithmic behavior. For all stages the sign of aT-MR($H\|c$) is positive, while the sign of cL-MR($H\|c$) is negative for the intermediate stages (3–5) and positive for low stages at low T and weak H.

Sugihara *et al.*[17] proposed a model to explain the above experimental results by assuming that the in-plane relaxation rate of interior G layers (Γ_i) is much larger than that of bounding G layers (Γ_b). (i) The c-axis resistivity ρ_c is formed of *series connections* of the c-axis resistivity contribution $\rho_c(G_bIG_b), \rho_c(G_bG_i), \rho_c(G_iG_{i+1}), \ldots$ along the c axis. The resistivities $\rho_c(G_bIG_b)$, $\rho_c(G_bG_i)$, and $\rho_c(G_iG_{i+1})$ are proportional to $(m_b\hbar/\Gamma_b)^{-1}$, $(m_b\hbar/\Gamma_b + m_i\hbar/\Gamma_i)^{-1}$, and $(m_i\hbar/\Gamma_i)^{-1}$, respectively. m_b and m_i are the effective mass of carriers in the bounding graphite (G_b) and interior graphite (G_i) layers. Since $\Gamma_i \gg \Gamma_b$, $\rho_c(G_iG_{i+1})$ is much larger than $\rho_c(G_bIG_b)$. This implies that the G_i layers form a bottleneck to c-axis conduction. The T dependence of ρ_c mainly comes from that of the bottleneck resistivity. (ii) The in-plane resistivity ρ_a is formed of *parallel connections* of the in-plane resistivity contributions $\rho_a(G_b)$ and $\rho_a(G_i)$, which are proportional to $(m_b\hbar/\Gamma_b)^{-1}$ and $(m_i\hbar/\Gamma_i)^{-1}$, respectively. So carriers are able to conduct mainly in the G_b layers, getting out of the bottleneck. Thus the T dependence of ρ_a mainly comes from that of the in-plane resistivity of G_b layers.

When the 2D WLE occurs in the G_i layers, not in the G_b layers, both a logarithmic behavior and N-MR are predicted to appear only in ρ_c. So far the logarithmic behavior and N-MR have been found in $CuCl_2$, $CoCl_2$, and $SbCl_5$ GIC's based on carbon fibers.[18–21] These behaviors have been discussed in terms of 2D WLE. As far as we know, however, it has not been shown through these studies that the G_i layers plays a significant role for c-axis conduction, partly because of the lack of data for c-axis resistivity of acceptor GIC's with various stages.

In this paper we have undertaken an extensive study on

the T and H dependences of ρ_c for a stage-4 $MoCl_5$, GIC, where the magnetic field is applied along the c axis. The observed logarithmic behavior in ρ_c and N-MR in $\rho_c(T,H)$ will be discussed in terms of a theory on 2D WLE.[22]

II. THEORETICAL BACKGROUND

We present a brief review on the theory of 2D WLE,[22,23] taking into account the case of a stage-4 $MoCl_5$ GIC. There are two different relaxation times of the carriers: the elastic lifetime τ_0 and the inelastic lifetime τ_ε. The usual Boltzmann theory neglects interference between the scattered partial waves and assumes that the momentum of the electron wave disappears exponentially after a time τ_0. This assumption yields the simple Drude formula for conductivity, σ_B^{2D} $(=N_{2D}e^2\tau_0/m)$, with a 2D carrier density N_{2D}. The weak-localization effect in the 2D disordered systems is essentially caused by quantum interference of the conduction electrons on system defects. The phase of the electron wave is maintained over the distance L_ε associated with inelastic scattering. When L_0 is the mean free path associated with elastic scattering $(L_0 \ll L_\varepsilon)$, the correction term in the 2D conductivity due to localization can be described by

$$\Delta\sigma_{2D} = -\frac{e^2}{\pi^2\hbar}\ln\left(\frac{L_\varepsilon}{L_0}\right). \tag{1}$$

When the relaxation time for inelastic scattering τ_ε is described by $1/\tau_\varepsilon \approx T^p$ and $L_\varepsilon = (D\tau_\varepsilon)^{1/2}$, the correction term has a logarithmic behavior

$$\Delta\sigma_{2D} = \frac{e^2}{2\pi^2\hbar}p\ln\left(\frac{T}{T_0}\right), \tag{2}$$

where D is the diffusion constant, T_0 is a characteristic temperature, and $e^2/2\pi^2\hbar = 1.233\,14\times10^{-5}\,\Omega^{-1}$.

In a uniform magnetic field H applied along the c axis, the localization effect is weakened. The magnetic field acts against the cancellation of two electron waves with opposite wave vectors $\mathbf{k}$ and $-\mathbf{k}$. The correction term to the 2D conductivity due to the 2D WLE depends on three characteristic lengths: a magnetic length $L_B = (c\hbar/eH)^{1/2}$, L_0, and L_ε. The magnetic length is the radius of the lowest cyclotron orbit. Under the condition that

$$L_0 \ll L_B \ll L_\varepsilon, \tag{3}$$

the change in the correction term of the 2D conductivity due to H is described by

$$\Delta\sigma_{2D} = -\frac{e^2}{\pi^2\hbar}\ln\left(\frac{L_B}{L_0}\right) = \frac{e^2}{2\pi^2\hbar}\ln H, \tag{4}$$

which increases with H, representing N-MR.

In the intermediate stages, the density of states of the G_i layer is small compared to that of the G_b layers, because the Fermi level is found near the bottom of the energy band. The diffusion length L_ε becomes long enough, and condition (3) can be satisfied. In the transition between the G_b layers, on the other hand, the density of states of the G_b layers is too large for condition (3) to be satisfied. Hence it does not contribute to the logarithmic behavior and N-MR.

If the spin-orbit scattering and scattering by magnetic impurities are also taken into account, the conductivity in the presence of H is of the form[22]

$$\Delta\sigma^{2D}(T,H) = -\frac{e^2}{2\pi^2\hbar}\left[\Psi\left(\frac{1}{2}+\frac{H_1}{H}\right) - \frac{3}{2}\Psi\left(\frac{1}{2}+\frac{H_2}{H}\right) + \frac{1}{2}\Psi\left(\frac{1}{2}+\frac{H_3}{H}\right)\right], \tag{5}$$

which is valid even at $H=0$. Here $\Psi(x)$ is the digamma function which has limiting forms as $\Psi(1/2+x) = \ln(x) + 1/24x^2$ for $x \gg 1$ and $\Psi(1/2) = -1.9635$; $H_1 = H_0 + H_{so} + H_s$, $H_2 = 4H_{so}/3 + 2H_s/3 + H_\varepsilon$, and $H_3 = 2H_s + H_\varepsilon$. The characteristic field H_k is related to the characteristic relaxation time τ_k by $H_k = c\hbar/4eD\tau_k$, where the index k stands for the following scattering process: 0 is elastic scattering, ε is inelastic scattering, s is magnetic scattering, and so is spin-orbit scattering. Since τ_ε is much larger than τ_0, H_0 is much larger than H_ε, leading to the inequality $H_1 \gg H_2$ and $H_1 \gg H_3$. For $H \ll H_1$, $\Delta\sigma^{2D}(T,H)$ is given by

$$\Delta\sigma^{2D}(T,H) = -\frac{e^2}{2\pi^2\hbar}\left[-\frac{3}{2}\Psi\left(\frac{1}{2}+\frac{H_2}{H}\right) + \frac{3}{2}\ln\left(\frac{H_2}{H}\right) + \frac{1}{2}\Psi\left(\frac{1}{2}+\frac{H_3}{H}\right) - \frac{1}{2}\ln\left(\frac{H_3}{H}\right)\right], \tag{6}$$

except for the H-independent term. When a function $f(x)[=\ln(1/x) - \Psi(1/2+1/x)]$ is newly introduced, $\Delta\sigma^{2D}(T,H)$ can be expressed by

$$\Delta\sigma^{2D}(T,H) = -\frac{e^2}{2\pi^2\hbar}\left[\frac{3}{2}f\left(\frac{H}{H_2}\right) - \frac{1}{2}f\left(\frac{1}{\xi}\frac{H}{H_2}\right)\right], \tag{7}$$

where a parameter ξ is defined by $\xi = H_3/H_2$. Equation (7) can be approximated as

$$\Delta\sigma^{2D}(T,H) = \frac{e^2}{96\pi^2\hbar}\left(3-\frac{1}{\xi^2}\right)\left(\frac{H}{H_2}\right)^2$$

for $H \ll H_2$, and

$$\Delta\sigma^{2D}(T,H) = \frac{e^2}{2\pi^2\hbar}\left[\ln\left(\frac{H}{H_2}\right) + \frac{1}{2}\ln\xi - 1.9635\right]$$

for $H_2 \ll H \ll H_0$.

III. EXPERIMENTAL PROCEDURE

The c-axis resistivity was measured using a superconducting quantum interference device magnetometer (Quantum Design, MPMS XL-5) with an external device control and an ultra-low-field capability option. Before inserting a sample at 298 K, the remanent magnetic field in a superconducting magnet was reduced to less than 3 mOe using the ultra-low-field capability option. For convenience, hereafter this remanent field is referred to as $H=0$. The sample was cooled down to 1.9 K in 8 h for an annealed system and 0.5 h for a quenched system. Then the c-axis resistivity was measured with increasing T from 1.9 to 50 K, with and without an external magnetic field along the c axis.

The c-axis resistivity was measured using a conventional

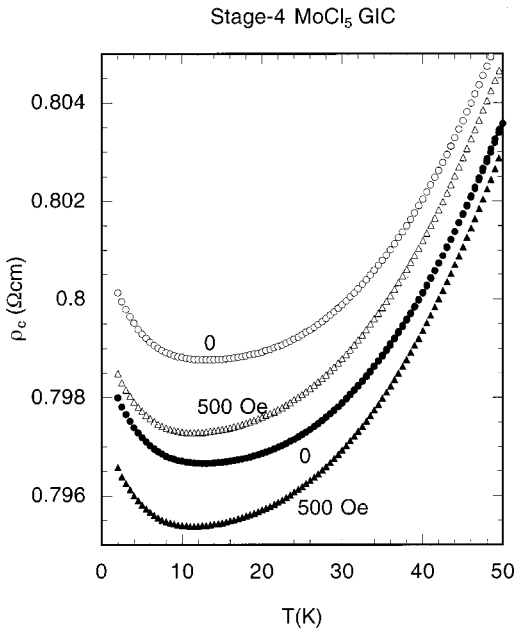

FIG. 1. T dependence of ρ_c for a stage-4 $MoCl_5$ GIC in the annealed (●, ▲) and quenched states (○, △). $H=0$(●,○) and 500 (▲, △). $H\|c$.

four-probe method. The sample has a rectangular form with typically a base 5×5 mm^2 and a height 0.5 mm along the c axis. Two thin gold wires (25-μm diameter) as the current and voltage probes were attached to the c surfaces of the sample by silver paste (4922N, du Pont). The current (10 mA) was supplied to the current probes by a programmable current source (Keithley, Model 224). The voltage across the voltage probes was measured by a digital nanovoltmeter (Keithley, Model 181).

IV. RESULT

Figure 1 shows the T dependence of ρ_c at $H=0$ and 500 Oe for a stage-4 $MoCl_5$ GIC for both the annealed and quenched systems, where H is along the c axis. The value of ρ_c for the quenched system is larger than the value of ρ_c for the annealed system at the same T and H. This feature reflects the degree of disorder in the graphite layers generated during the cooling process. Figures 2(a) and 2(b) show the T dependence of ρ_c for the annealed system in the presence of H along the c axis. A similar behavior is observed for the quenched system. The resistivity ρ_c decreases with increasing T at low T, showing a local minimum at a temperature $T_{\min}$, and increases with further increasing T. Figure 3 shows the H dependence of $T_{\min}$ for both the annealed and quenched systems. The temperature $T_{\min}$ decreases with increasing H at low H, exhibiting a local minimum around $H=2$ kOe, and increases with further increasing H: $T_{\min}=46$ K at $H=20$ kOe.

In order to analyze the T dependence of ρ_c in the presence of H, we assume that the resistivity is described by

$$\rho_c=\rho_0-\rho_1\ln(T)+\rho_2T+\rho_3T^2, \tag{8}$$

where ρ_0, ρ_1, ρ_2, and ρ_3 are positive constants dependent on H, the second logarithmic term is due to the 2D WLE,

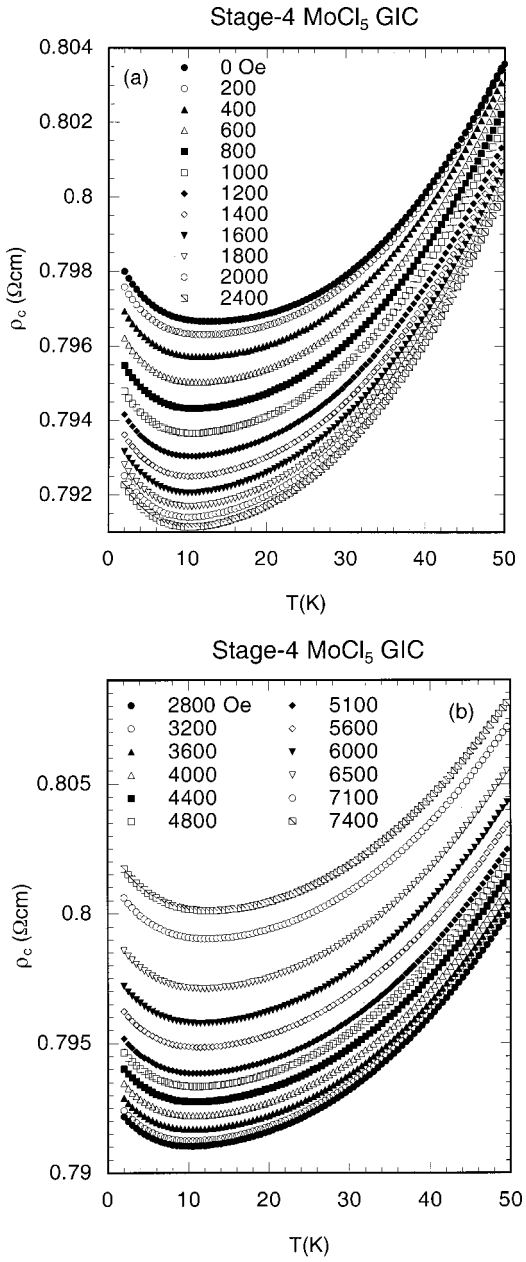

FIG. 2. (a) and (b) T dependence of ρ_c with various H's for a stage-4 $MoCl_5$ GIC in the annealed state. $H\|c$.

and the third and fourth terms are due to the scattering of carriers by phonons.[24] The value of $T_{\min}$ can be calculated from $d\rho_c/dT=0$ as

$$T_{\min}=(\sqrt{\rho_2^2+8\rho_1\rho_3}-\rho_2)/4\rho_3. \tag{9}$$

We find that ρ_c vs T with $1.9\leqslant T\leqslant25$ K for both the annealed and quenched systems can be also well described by Eq. (8) for each H below 5.6 kOe. The parameters ρ_0 to ρ_3 for each H are determined by a least squares fit of the data to Eq. (8): for example, $\rho_0=0.79869\pm0.00001\,\Omega$ cm, $\rho_1=(1.038\pm0.024)\times10^{-3}\,\Omega$ cm, $\rho_2=(1.863\pm0.534)\times10^{-5}\,\Omega\,\mathrm{cm\,K^{-1}}$, and $\rho_3=(2.269\pm0.120)\times10^{-6}\,\Omega\,\mathrm{cm\,K^{-2}}$ at $H=0$ for the annealed system. The corresponding fitting curve is denoted by the solid line in Fig. 4. In Fig. 3 we also show the calculated values of $T_{\min}$ for both the annealed and quenched systems. These values are ob-

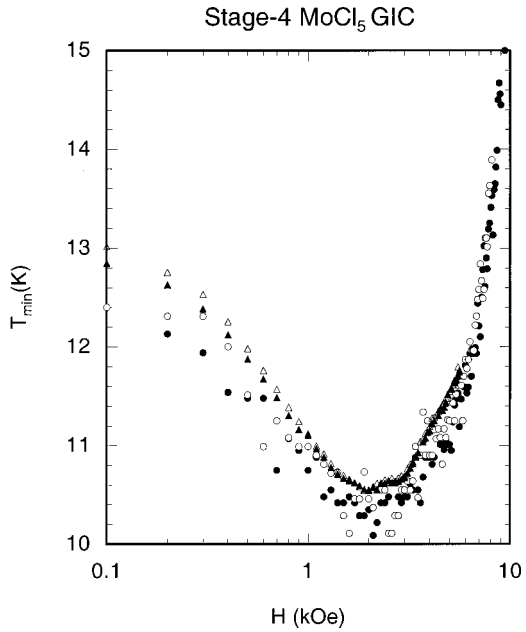

FIG. 3. H dependence of $T_{\min}$. Values of $T_{\min}$ experimentally observed in the annealed state (●) and the quenched state (○). Calculated values of $T_{\min}$ in the annealed state (▲) and the quenched state (△).

tained using parameters ρ_1 to ρ_3 for each H. The experimental data $T_{\min}$ vs H are in good agreement with the calculated results.

Figure 5 shows the H dependence of the ratio ρ_1/ρ_0 for annealed and quenched systems. The ratio ρ_1/ρ_0 tends to increase slightly with increasing H: $\rho_1/\rho_0=0.0013$ at $H=0$ to 0.001 38 at $H=5.6$ kOe for the annealed system. This is in contrast with the case of a $CuCl_2$ GIC based on pitch-derived carbon fiber: the ratio ρ_1/ρ_0 shows a drastic decrease at low H (<2 kOe) and saturates at high H.[20] In a

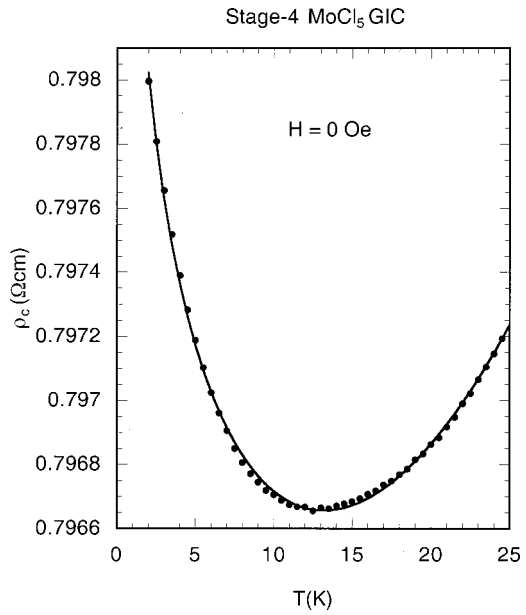

FIG. 4. T dependence of ρ_c for a stage-4 $MoCl_5$ GIC in the annealed state. $H=0$. The solid line denotes a least-squares fitting curve described by Eq. (8).

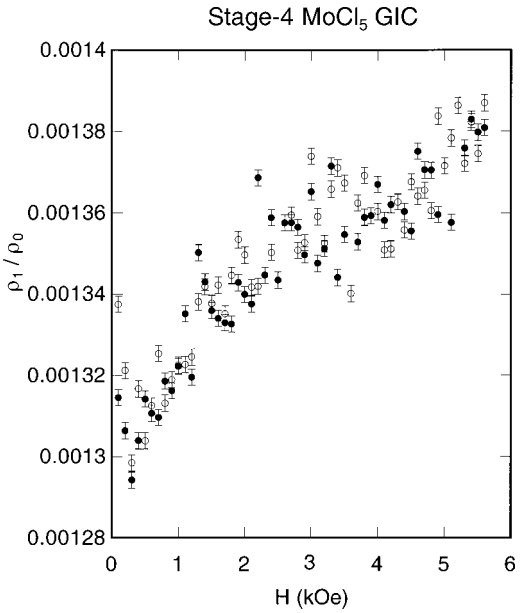

FIG. 5. H dependence of ratio ρ_1/ρ_0 for a stage-4 $MoCl_5$ GIC in the annealed (●) and quenched states (○).

previous paper[9] we showed that the following relation is valid in a stage-4 $MoCl_5$ GIC:

$$\frac{\rho_1}{\rho_0}=\frac{e^2}{2\pi^2\hbar}\frac{C}{\sigma_{2D}^0}, \tag{10}$$

where C is a constant, $\sigma_{2D}^0(=1.0776\times10^{-2}\,\Omega^{-1})$ corresponds to the in-plane conductivity defined by I_c/ρ_a^0, ρ_a^0 ($\approx18\ \mu\Omega$ cm at 4.2 K)[11] is the in-plane resistivity, and $I_c(19.396\pm0.014\,\text{Å})$ is the c-axis repeat distance for the stage-4 $MoCl_5$ GIC. Using the ratio $\rho_1/\rho_0=1.30\times10^{-3}$, the constant C can be estimated as 1.14, which is comparable with 0.90 in a previous paper.[9]

Figures 6(a) and 6(b) show the H dependence of ρ_c with $1.9\leqslant T\leqslant50$ K for the annealed system. For each T, ρ_c decreases with increasing H at low H, exhibits a local minimum around $H=2.5$ kOe, and increases with further increasing H. The sign of the difference $\Delta\rho_c[=\rho_c(T,H)-\rho_c(T,H=0)]$ is negative for $0\leqslant H\leqslant6-7$ kOe due to the 2D WLE. Because of the Boltzmann term σ_B^{2D}, which may drastically decrease with increasing H above 6–7 kOe, the sign of $\Delta\rho_c$ becomes positive. We find that the H dependence of ρ_c for high $H(10\leqslant H\leqslant44$ kOe) is given by

$$\rho_c=a_0+a_1H^{\alpha}, \tag{11}$$

with an exponent $\alpha=1.007\pm0.002$, which is almost independent of T for $1.9\leqslant T\leqslant50$ K [see Fig. 6(b)]. In contrast, for low H ($0.6\leqslant H\leqslant2.0$ kOe) the H dependence of ρ_c is given by a logarithmic term

$$\rho_c=b_0-b_1\ln(H), \tag{12}$$

due to the 2D WLE. The ratio b_1/b_0 is dependent on T. It decreases with increasing T: $b_1/b_0=(3.93\pm0.05)\times10^{-3}$ at 1.9 K and $(2.14\pm0.05)\times10^{-3}$ at 50 K. Note that the ratio b_1/b_0 is roughly 2–4 times as large as the ratio ρ_1/ρ_0.

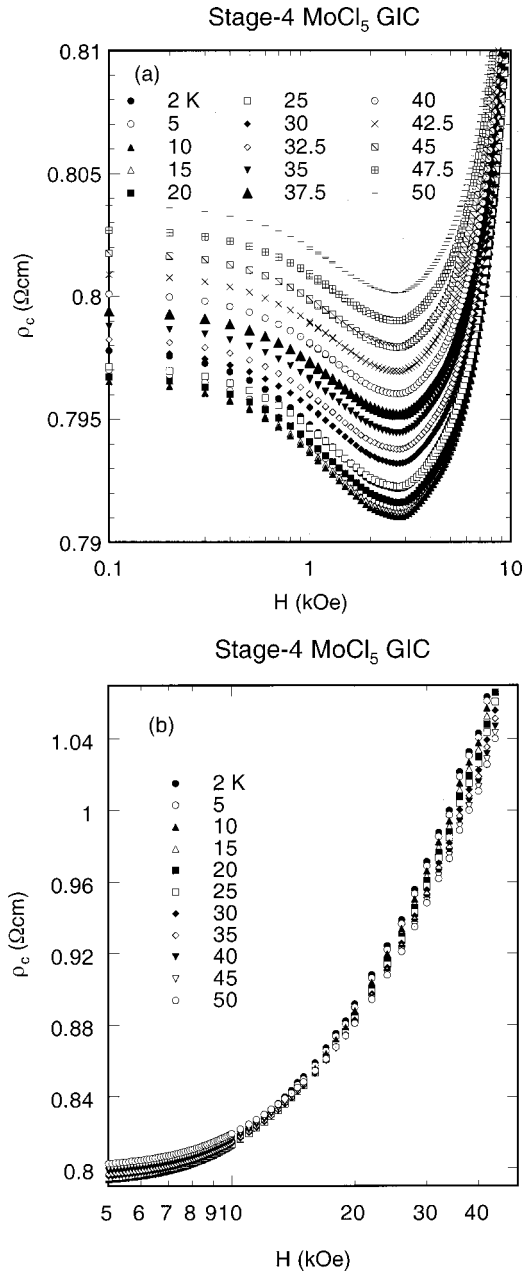

FIG. 6. (a) and (b) H dependence of ρ_c for a stage-4 $MoCl_5$ GIC in the annealed state at various T's $H \| c$.

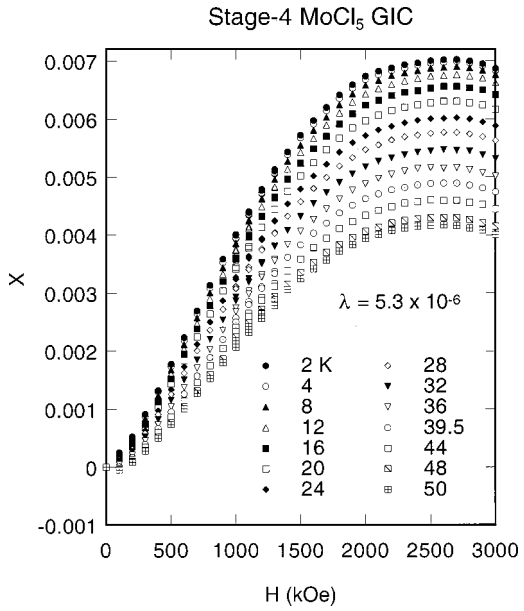

FIG. 7. H dependence of $X[=\Delta\sigma(T,H)/\sigma(T,H=0)]$ with $\lambda = 5.3\times10^{-6}$ for various T's.

V. DISCUSSION

A. Derivation of conductivity tensor

As described in Sec. I, we assume that the c-axis resistivity of a stage-4 $MoCl_5$ GIC is proportional to the in-plane resistivity tensor of the G_i layers (ρ_{xx}), where $\rho_{xx}=A\rho_c$ and A is constant. Then the conductivity tensor σ_{xx} in the G_i layers can be expressed as

$$\sigma_{xx}=\frac{1}{A\rho_c}\frac{1}{1+\left(\frac{R_H H}{A\rho_c}\right)^2}, \tag{13}$$

where the Hall coefficient R_H is defined by

$$R_H=\frac{1}{nec}=\frac{6.25\times10^{10}}{n}(\Omega\ \text{cm/Oe}), \tag{14}$$

and n is the carrier density per cm^3. In the frame of the Blinowski-Rigaux 2D electronic band model,[25] the effective mass m^* and the 2D carrier density N_{2D} are independent of the kind of acceptor GIC's for a given Fermi energy: typically $m^*=0.25m_0$ and $N_{2D}=10^{14}/cm^2$ (Piraux *et al.*[20]). The carrier density n for a stage-4 $MoCl_5$ GIC is related to N_{2D} by $n=N_{2D}/I_c$. Since $I_c=19.396\pm0.014$ Å, n is estimated as $5.16\times10^{20}/cm^3$. Here we introduce a parameter λ defined by $\lambda=R_H/A$. Using the value of $A(A=\rho_a/\rho_c=18\,\mu\Omega\ \text{cm}/0.8\ \Omega\ \text{cm}=2.25\times10^{-5})$, we have $\lambda=6.25\times10^{10}/An=5.39\times10^{-6}$. Then the correction term in the conductivity (X) can be rewritten as

$$X=\frac{\Delta\sigma(T,H)}{\sigma(T,H=0)}=\frac{\rho_c(T,H=0)}{\rho_c(T,H)}\frac{1}{1+\frac{\lambda^2H^2}{[\rho_c(T,H)]^2}}-1. \tag{15}$$

Experimentally we determine the value of λ for a stage-4 $MoCl_5$ GIC as follows. First we calculate the H dependence of X for $1.9\leqslant T\leqslant50$ K when the parameter λ is changed between $\lambda=2\times10^{-6}$ and 2×10^{-5} around the expected value $\lambda=5.39\times10^{-6}$. For each λ we find that the H dependence of X at $T=2.0$ K in the limited field range between 0.5 and 2 kOe can be well fitted to a logarithmic form defined by $c_1+c_2\ln(H)$. Then we make a plot of c_2 as a function of λ. The value of c_2 linearly decreases with λ for $3\times10^{-6}\leqslant\lambda\leqslant7\times10^{-6}$: $c_2=0.00413-37.65\ \lambda$. An appropriate value of λ ($=5.30\times10^{-6}$) is chosen under the condition that c_2 coincides with the value b_1/b_0 ($=3.93\pm0.05)\times10^{-3}$ at 1.9 K. This value of λ is very close to the expected value ($=5.39\times10^{-6}$).

Figure 7 shows the H dependence of X with $\lambda=5.30\times10^{-6}$ at various T's. The value of X is positive at least below 7–8 kOe, and has a peak around $H=2.6$–2.7 kOe.

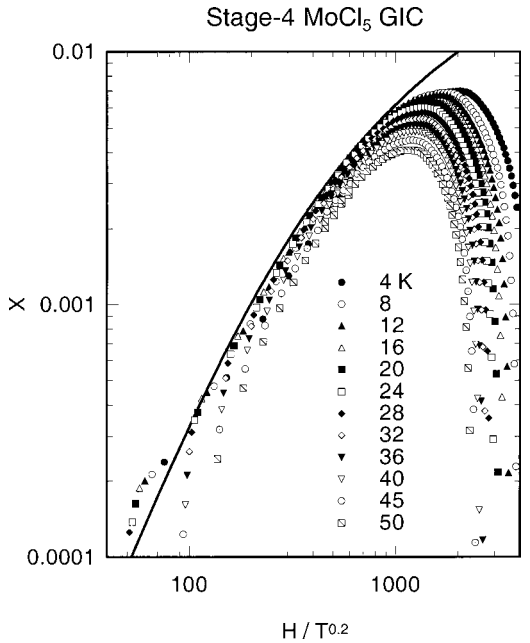

FIG. 8. Scaling plot of X with $\lambda=5.3\times10^{-6}$ as a function of H/T^p ($p=0.2$) for various T's. The solid line is described by Eq. (18).

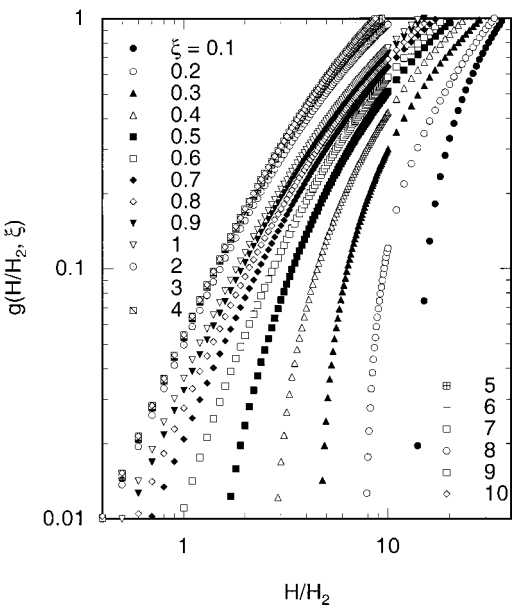

FIG. 9. Plot of $g(H/H_2,\xi)$ given by Eq. (16) as a function of H/H_2, where the parameter ξ is changed between 0.1 and 10.

These two features are independent of T for $1.9\leqslant T\leqslant 50$ K. For any fixed H the value of X decreases with increasing T. Figure 8 shows the log-log plot of X with $\lambda=5.30\times10^{-6}$ as a function of H/T^p with $p=0.2$, where p is the exponent of $\tau_\varepsilon:\tau_\varepsilon\approx T^{-p}$. This value of p is much smaller than that ($p=1$ or 2) derived from the T dependence of ρ_c at high T for a stage-4 $MoCl_5$ GIC. It is well described by the third ($\rho_2 T$) and fourth terms ($\rho_3 T^2$) in Eq. (8). This may suggest that τ_ε, the dephasing time due to inelastic scattering is rather different from the transport relaxation time.

B. Scaling relation of conductivity

Here we discuss the H and T dependences of the conductivity X in terms of Eq. (7) predicted from the theory of 2D WLE. In Fig. 9 we show a log-log plot of the normalized conductivity defined by

$$g\left(\frac{H}{H_2},\xi\right)=\frac{\Delta\sigma^{2D}(T,H)}{\dfrac{e^2}{2\pi^2\hbar}}=-\frac{3}{2}f\left(\frac{H}{H_2}\right)+\frac{1}{2}f\left(\frac{1}{\xi}\frac{H}{H_2}\right), \tag{16}$$

as a function of H/H_2, when ξ, given by

$$\xi=\frac{H_3}{H_2}=\frac{2H_s+H_\varepsilon}{4H_{so}/3+2H_s+H_\varepsilon}, \tag{17}$$

is changed as a parameter. When ξ is smaller than $1/\sqrt{3}$ ($=0.577$), the normalized conductivity becomes negative at small H/H_2, showing a local minimum. It increases with further increasing H/H_2 and becomes saturated at high H/H_2. Note that this negative part of normalized conductivity is not shown in Fig. 9. In contrast, for $\xi>1/\sqrt{3}$ the normalized conductivity is positive for all the values of H/H_2. It increases with increasing H/H_2.

Here we consider the special case ($H_s=H_{so}=0$), which may be the case for a stage-4 $MoCl_5$ GIC. The spin-orbit interaction may be neglected because no negative X is observed for low H. The magnetic interaction may be negligibly weak in spite of the possible existence of Mo^{5+} spins ($S=\frac{1}{2}$) in the $MoCl_5$ layers because the 2D WLE occurs mainly in the G_i layers. Then the normalized conductivity is predictably expressed by a function $f(H/H_\varepsilon)$, where H/H_ε is proportional to H/T^p since $H_\varepsilon=\hbar/(4eD\tau_\varepsilon)$, and τ_ε is proportional to T^{-p}. We find that such a scaling relation is confirmed from the T and H dependence of X with $\lambda=5.3\times10^{-6}$. As shown in Fig. 8 it seems that almost all the data of X with $T<34$ K fall on the solid line described by a scaling function

$$X=-X_0 f\left(\frac{H}{H_\varepsilon}\right) \tag{18}$$

for $H/T^{0.2}<800$, where $X_0\approx0.0074$ and $H_\varepsilon=\beta T^p$ with $p=0.20\pm0.02$ and $\beta\approx90$. For $H/T^{0.2}\gg800$ the data of X greatly deviate from this scaling function partly because of the 2D Boltzmann term σ_B^{2D}. The characteristic field H_ε is on the order of 100 Oe at $T=2$ K. Here we note that the data of X with $34<T<50$ K seem to agree with a function given by Eq. (16), with ξ slightly smaller than 1. As shown in Fig. 9 the normalized conductivity exhibits a parallel shift to the higher side of H/H_2 when ξ is slightly smaller than 1. This may suggest that our assumption ($H_{so}=H_s=0$ and $H_\varepsilon=\beta T^p$) is not always valid at high temperatures.

As pointed out in a previous paper,[11] the possibility of the Kondo effect as a cause for the logarithmic behavior and N-MR of ρ_c can be ruled out for the following reasons. Since the Kondo effect is an isotropic effect, the N-MR should be independent of the direction of H. In fact the N-MR can be observed only for H parallel to the c axis. The N-MR should appear in a stage-2 $MoCl_5$ GIC because of the relatively strong exchange interactions between spins of carriers in the G_b layers and the Mo^{5+} spins in the nearest neighbor I layer.

In fact, $\rho_c(H)$ for stage 2 shows a positive MR over the whole T and H ranges examined.

VI. CONCLUSION

The T and H dependences of ρ_c for a stage-4 $MoCl_5$ GlC show a logarithmic temperature dependence of ρ_c at low T and a negative magnetoresistance at low H. These behaviors can be well described by the existing theories of weak localization in 2D disordered systems, under the assumption that $\tau_\varepsilon \ll \tau_{so}, \tau_s$. The 2D weak localization effect occurs mainly in the interior G layers, where the diffusion length L_ε associated with inelastic scattering satisfies the condition $L_0 \ll L_B \ll L_\varepsilon$. The observed behaviors are strongly dependent on the direction of H: the orbital motion of carriers in the interior G layers is influenced by the application of H along the c axis.

ACKNOWLEDGMENTS

The authors thank A. W. Moore for providing HOPG samples to them, and C. Lee and R. Niver for their help in sample preparation of the stage-4 $MoCl_5$ GlC. The work at Binghamton was partially supported by the Research Foundation of SUNY-Binghamton (Contract No. 240-9807A).

*Present address: Energy Laboratory, Electronic Research Center, Samsung Yokohama Research Institute, 2-7, Sugasawa-cho, Tsurumi-ku, Yokohama 230-0027, Japan.

[1] D. T. Morelli and C. Uher, Phys. Rev. B **27**, 2477 (1983).
[2] E. McRae, J. F. Mareche, A. Bendriss-Rerhrhaye, P. Lagrange, and M. Lelaurain, Ann. Phys. (Paris), Colloq. Suppl. 2, **11**, 13 (1986).
[3] J. F. Mareche, E. McRae, A. Bendriss-Rerhrhaye, and P. Lagrange, J. Phys. Chem. Solids **47**, 477 (1986).
[4] E. McRae, J. F. Mareche, M. Lelaurain, G. Furdin, and A. Hérold, J. Phys. Chem. Solids **48**, 957 (1987).
[5] E. McRae and J. Mareche, J. Mater. Res. **3**, 75 (1988).
[6] R. Powers, A. K. Ibrahim, G. O. Zimmerman, and M. Tahar, Phys. Rev. B **38**, 680 (1988).
[7] E. McRae, M. Lelaurain, J. F. Mareche, G. Furdin, A. Hérold, and M. Saint Jean, J. Mater. Res. **3**, 97 (1988).
[8] B. Sundqvist, O. E. Andersson, E. McRae, M. Lelaurain, and J. F. Mareche, J. Mater. Res. **10**, 436 (1995).
[9] M. Suzuki, C. Lee, I. S. Suzuki, K. Matsubara, and K. Sugihara, Phys. Rev. B **54**, 17 128 (1996).
[10] M. Suzuki, I. S. Suzuki, C. Lee, R. Niver, K. Matsubara, and K. Sugihara, J. Phys.: Condens. Matter **9**, 10 399 (1997).
[11] K. Matsubara, K. Sugihara, I. S. Suzuki, and M. Suzuki, J. Phys.: Condens. Matter **11**, 3149 (1999).
[12] K. Sugihara, Phys. Rev. B **29**, 5872 (1984).
[13] S. Shimamura, Synth. Met. **12**, 365 (1985).
[14] K. Sugihara, Phys. Rev. B **37**, 4752 (1988).
[15] K. Sugihara, J. Phys. Soc. Jpn. **62**, 624 (1993).
[16] K. Sugihara and K. Matsubara, Mol. Cryst. Liq. Cryst. **310**, 255 (1998).
[17] K. Sugihara, K. Matsubara, I. S. Suzuki, and M. Suzuki, J. Phys. Soc. Jpn. **67**, 4169 (1998).
[18] L. Piraux, J.-P. Issi, J-P. Michenaud, E. McRae, and J. F. Mareche, Solid State Commun. **56**, 567 (1985).
[19] L. Piraux, V. Bayot, J.-P. Michenaud, J.-P. Issi, J. F. Mareche, and E. McRae, Solid State Commun. **59**, 711 (1986).
[20] L. Piraux, V. Bayot, X. Gonze, J.-P. Michenaud, and J.-P. Issi, Phys. Rev. B **36**, 9045 (1987).
[21] L. Piraux, J. Mater. Res. **5**, 1285 (1990).
[22] S. Hikami, A. I. Larkin, and Y. Nagaoka, Prog. Theor. Phys. **63**, 707 (1980).
[23] P. A. Lee and T. V. Ramakrishnan, Rev. Mod. Phys. **57**, 287 (1985).
[24] H. Kamimura, K. Nakao, T. Ohno, and T. Inoshita, Physica B & C **99**, 401 (1980).
[25] J. Blinowski, Nguyen Hy Hau, C. Rigaux, J. P. Vieren, R. Le Toullec, G. Furdin, A. Herold, and J. Melin, J. Phys. (Paris) **41**, 47 (1980).